AIAA JOURNAL
Vol. 41, No. 12, December 2003

Optimum Control Voltage Design for Constrained Static Shape Control of Piezoelectric Structures

Dongchang Sun* and Liyong Tong†
University of Sydney, Sydney, New South Wales 2006, Australia

Design optimization of control voltage distribution for constrained static shape control of structures using piezoelectric actuators is investigated. Two cases are studied. In the first case, a scheme is developed to find the optimal control voltage distribution minimizing the square error between the desired and actuated shapes subject to a given control electric energy. The optimal control voltage constrained by control energy can be found after solving an algebraic equation in terms of the Lagrangian multiplier. An alternative form for this algebraic equation is derived by taking advantage of an eigenvalue problem of a real symmetrical matrix, which significantly reduces the computational cost for finding its roots. A procedure for finding the optimal control energy is also given. In the second case, a process of seeking the control voltage distribution with least control energy for any given square error tolerance between the actuated and desired shapes is presented. Finally, illustrative examples for the constrained shape control of thin plates are given to demonstrate the presented methods.

Nomenclature

E	=	control energy
e	=	square error
$\boldsymbol{f}$	=	force vector
$\boldsymbol{G}$	=	electric–mechanical coupling matrix
$\boldsymbol{K}$	=	stiffness matrix
m	=	dimension of generalized shape vector
n	=	number of mechanical degrees of freedom
n_V	=	numbers of electric degrees of freedom
$\boldsymbol{R}$	=	weighting matrix
$\boldsymbol{u}$	=	vector of nodal displacements
$\boldsymbol{v}$	=	vector of nodal voltages
$\boldsymbol{y}$	=	generalized shape vector
z_0	=	electric conductance
α	=	eigenvalue
ε	=	strain vector
λ	=	Lagrangian multiplier
φ	=	eigen vector
χ	=	curvature vector

I. Introduction

SHAPE control means control of position or alignment of some points on a structure to track desired values by applying proper forces provided by certain number of force actuators. Shape control has been applied to various systems, such as in large space truss structures,[1] adaptive mirrors,[2] antenna reflectors,[3] and adaptive variable camber wings[4] to correct their shape distortions introduced by in-orbit thermal distortion, gravity, and other disturbances. In recent years, piezoelectric actuators have been widely used to replace traditional force actuators in shape control of flexible structures.[5–8] Because the piezoelectric patches are very lightweight compared to the force actuators, a large number of such patches can be integrated in the structures to control their shapes more precisely.

In static shape control of a composite structure with piezoelectric actuators, the main task is to find the optimal control voltages exerted on the actuator to minimize the error between the desired and the actuated shapes, which can usually be converted to linear least-squares problems.[9,10] The methods used in determining the optimum control voltages for static shape control may be sorted into three categories. In the first category, the control voltages are determined based on finding analytical solution of the displacements of a structure to the actuating sources. Kapuria et al.[11] presented a three-dimensional exact solution for a simply supported cross-ply laminated finite cylindrical panel with some piezoelectric layers subjected to thermoelectromechanical load using a Fourier series method. Based on their solution, several actuating schemes for shape control of thermally loaded panel were investigated. Yang and Ngoi[12] gave the analytical solutions for a beam with piezoelectric actuator patches and examined the limitation of a small number of piezoelectric actuators in realizing precise shape control. The analytical solution is usually limited by a few special actuator configurations and boundaries. In the second category, the control voltages for the piezoelectric actuators are determined by theoretically finding the extremums for a set of objective functions. Koconis et al.[13] developed a solution technique to find the optimal control voltage by minimizing an error function between the deformed shape and the desired shape. The advantage for this category is that it does not need much computation to find the optimal voltage distribution, and its disadvantage is that it may not be suitable for indifferentiable objective functions. In the third category, the optimal control voltage for the given objective functions is iteratively sought using numerical optimization algorithms. Hsu et al.[14] used the gradient projection algorithm to find the optimal values of design variables in the shape control of plates. Onoda and Hanawa[15] used the genetic and simulating annealing methods to choose the optima locations of the actuators in static shape control. Agrawal and Treanor[16] employed the simplex search algorithm to find the optimal actuator locations and voltages and found that separately optimizing actuator locations and voltages could produce reliable results. Chee et al.[17] developed a perturbation buildup voltage distribution (PBVD) algorithm to find the optimal voltage distribution for a slope-displacement-based objective function. The methods in this category can be applied for almost all objective functions, but may be very time consuming particularly when a large number of actuators are used. More details on shape control of structures may be found in Irschik's recent review paper.[18]

Most current research on shape control of structures is limited to optimal voltage distribution and actuator locations only, and no constraints for control energy are imposed. It is well known that the control voltages for some actuators to achieve the desired shape can

Received 6 March 2003; revision received 5 August 2003; accepted for publication 7 August 2003. Copyright © 2003 by the American Institute of Aeronautics and Astronautics, Inc. All rights reserved. Copies of this paper may be made for personal or internal use, on condition that the copier pay the $10.00 per-copy fee to the Copyright Clearance Center, Inc., 222 Rosewood Drive, Danvers, MA 01923; include the code 0001-1452/03 $10.00 in correspondence with the CCC.

*Australian Research Council Research Associate, School of Aerospace, Mechanical and Mechatronic Engineering; dsun@aeromech.usyd.edu.au.

†Associate Professor, School of Aerospace, Mechanical and Mechatronic Engineering; ltong@aeromech.usyd.edu.au. Senior Member AIAA.

be very high for a given actuator configurations. The high voltage will make the optimal voltage distribution impractical because it can cause depolarization of the piezoelectric actuators or even damage the entire actuating system. Therefore, the control energy consumption should be considered in practical designs for shape control of structures, and its effect on the voltage distribution should be investigated.

In engineering applications, we are particularly concerned with two types of problems on static shape control of structures. In the first problem, the control precision is the prime concern, and the main purpose of the shape control is to make the actuated shape as close as possible to the desired one, while the control electric energy is limited. Hence, the solution of this problem means finding the optimal control voltage distribution among the actuators whose energy is within the permissive range so as to minimize the difference between the actuated and desired shapes. In the second problem, the control electric energy is the major concern, and the objective is to find the least control energy while ensuring that the difference between the actuated and desired shapes falls within a prescribed range. The task for this problem is to find the control voltages with least electric energy capable of limiting the difference of the actuated and desired shapes within a given range. Both problems are related to control electric energy and the difference measure between the actuated and desired shapes and are defined as constrained static shape control of flexible smart structures, which are addressed in this paper. First, a scheme for finding the optimum control voltages subject to given control energy is presented. The optimum control voltage with given control energy that minimizes a generalized shape closeness index can be obtained after solving an algebraic equation. An efficient form of this algebraic equation of the unknown Lagrangian multiplier is derived so that the computing time required to find its roots is greatly reduced. Second, an analytical method for the optimum control energy, as well as the voltage distribution, is developed to achieve a desired shape within a given square error tolerance. Simulation examples for constrained static shape control of a thin plate are given based on a finite element modeling using an adhesive element between the host plate and the actuator.

II. Basic Equations for Static Shape Control of Smart Structures

The static global actuation equations of a smart structure with piezoelectric actuators based on finite element analysis (FEA) can be expressed in the following form:

$$\boldsymbol{Ku} + \boldsymbol{Gv} = \boldsymbol{f} \tag{1}$$

where $\boldsymbol{K} \in R^{n \times n}$ is the global stiffness matrix, $\boldsymbol{G} \in R^{n \times n_V}$ is a electric–mechanical coupling matrix due to the piezoelectricity of the piezoelectric actuators, $\boldsymbol{u} \in R^n$ is the displacement vector consisting of all nodal displacements, $\boldsymbol{v} \in R^{n_V}$ is the voltage vector composed of all nodal voltage of the piezoelectric actuators, $\boldsymbol{f} \in R^n$ is the force vector contributed by all mechanical loads. As a special case where the control voltage is uniformly applied on each piezoelectric actuator, the number of electric degrees of freedom (DOF) is equal to that of the piezoelectric actuators.

One primary task of shape control of a smart structure is to find a voltage distribution for the piezoelectric actuators that can actuate the structure and change its shape to a desired one. Naturally, the shape of a structure is usually described by its displacements from a selected reference system, and static shape control aims to find a suitable control voltage $\boldsymbol{v}$ that makes the actual displacement $\boldsymbol{u}$ equal or close to the desired $\boldsymbol{u}_d$. More generally, we consider a generalized shape defined by

$$\boldsymbol{y} = \boldsymbol{Ru} \tag{2}$$

where $\boldsymbol{R} \in R^{m \times n}$ is a weighting matrix, and $\boldsymbol{y} \in R^m$ is an index vector, which may be displacement, slope,[17] curvature,[19] strain, generalized force, or even their combination depending on the selection of the weighting matrix. The curvatures, strains, and generalized force of a structure can be expressed in term of the displacements

$$\boldsymbol{\chi} = \boldsymbol{B}_c\boldsymbol{u}, \qquad \boldsymbol{\varepsilon} = \boldsymbol{B}_s\boldsymbol{u}, \qquad \boldsymbol{f}_g = \boldsymbol{K}_g\boldsymbol{u} \tag{3}$$

where $\boldsymbol{B}_c$, $\boldsymbol{B}_s$, and $\boldsymbol{K}_g$ are coefficient matrices for curvatures, strains, and generalized forces, respectively. When the translational displacements, rotational angles (slopes), curvatures, strains (or stress), and generalized forces are considered in the shape control, a multiobjective shape $\boldsymbol{y}$ with different weighting coefficients can be written as

$$\boldsymbol{y} = \boldsymbol{R}_d\boldsymbol{u} + \boldsymbol{R}_c\boldsymbol{\chi} + \boldsymbol{R}_s\boldsymbol{\varepsilon} + \boldsymbol{R}_g\boldsymbol{f}_g = \boldsymbol{Ru} \tag{4}$$

where $\boldsymbol{R}_d$, $\boldsymbol{R}_c$, $\boldsymbol{R}_s$, and $\boldsymbol{R}_g$ are the weighting matrices for the displacements including both translational and rotational, curvatures, strains, and generalized forces, respectively. Substituting Eq. (3) into Eq. (4) yields the following overall weighting matrix:

$$\boldsymbol{R} = \boldsymbol{R}_d + \boldsymbol{R}_c\boldsymbol{B}_c + \boldsymbol{R}_s\boldsymbol{B}_s + \boldsymbol{R}_g\boldsymbol{K}_g \tag{5}$$

As a special case where the translational and rotational displacements of a structure are the main concern, the weighting matrix $\boldsymbol{R}$ is equal to $\boldsymbol{R}_d$, and it can be selected as

$$\boldsymbol{R}_d = \begin{bmatrix} \boldsymbol{R}_1 & \boldsymbol{0} & \boldsymbol{0} & \boldsymbol{0} & \boldsymbol{0} & \boldsymbol{0} \\ \boldsymbol{0} & \boldsymbol{R}_2 & \boldsymbol{0} & \boldsymbol{0} & \boldsymbol{0} & \boldsymbol{0} \\ \boldsymbol{0} & \boldsymbol{0} & \ddots & \boldsymbol{0} & \boldsymbol{0} & \boldsymbol{0} \\ \boldsymbol{0} & \boldsymbol{0} & \boldsymbol{0} & \boldsymbol{R}_i & \boldsymbol{0} & \boldsymbol{0} \\ \boldsymbol{0} & \boldsymbol{0} & \boldsymbol{0} & \boldsymbol{0} & \ddots & \boldsymbol{0} \\ \boldsymbol{0} & \boldsymbol{0} & \boldsymbol{0} & \boldsymbol{0} & \boldsymbol{0} & \boldsymbol{R}_N \end{bmatrix} \tag{6}$$

where N is the total number of nodes and $\boldsymbol{R}_i$ is a subweighting matrix related to the DOFs for each node. For example, for a FEA model based on the first-order shear deformation plate theory, the subweighting matrix has the form

$$\boldsymbol{R}_i = \begin{bmatrix} R_{ui} & 0 & 0 & 0 & 0 \\ 0 & R_{vi} & 0 & 0 & 0 \\ 0 & 0 & R_{wi} & 0 & 0 \\ 0 & 0 & 0 & R_{\theta i} & 0 \\ 0 & 0 & 0 & 0 & R_{\varphi i} \end{bmatrix}, \qquad i = 1, 2, \ldots, n \tag{7}$$

where R_{ui}, R_{vi}, R_{wi}, $R_{\theta i}$, and $R_{\varphi i}$ are the weighting coefficients for the translational displacements in x and y, directions, and rotational angles about the x and y axes, respectively, for the ith node. For example, Chee et al.[17] chose $R_{ui} = R_{vi} = 0$ and allowed R_{wi} and $R_{\theta i}$, $R_{\varphi i}$ to be independent weighting factors.

For a given desired shape $\boldsymbol{y}_d \in R^m$, the error between the actual shape and the desired shape can be measured by the square error e defined by

$$e = (\boldsymbol{y} - \boldsymbol{y}_d)^T(\boldsymbol{y} - \boldsymbol{y}_d) \tag{8}$$

The control energy consumed by the piezoelectric actuators is abstractly defined as

$$E = z_0\boldsymbol{v}^T\boldsymbol{v} \tag{9}$$

where z_0 is a weighting coefficient representing electric conductance.

Without loss of generality, the stiffness matrix $\boldsymbol{K}$ is assumed to be nonsingular, and therefore, the relationship between the displacement and control voltage can be expressed as

$$\boldsymbol{u} = -\boldsymbol{K}^{-1}\boldsymbol{Gv} + \boldsymbol{K}^{-1}\boldsymbol{f} \tag{10}$$

Substituting Eq. (10) into Eqs. (2) and (8) gives

$$e = \boldsymbol{v}^T\boldsymbol{Av} + 2\boldsymbol{v}^T\boldsymbol{By}_d - 2\boldsymbol{v}^T\boldsymbol{Cf} + \boldsymbol{f}^T\boldsymbol{Df} - 2\boldsymbol{y}_d^T\boldsymbol{Pf} + \boldsymbol{y}_d^T\boldsymbol{y}_d \tag{11}$$

where

$$\boldsymbol{A} = \boldsymbol{G}^T\boldsymbol{K}^{-T}\boldsymbol{R}^T\boldsymbol{R}\boldsymbol{K}^{-1}\boldsymbol{G} \in R^{n_V \times n_V}, \qquad \boldsymbol{B} = \boldsymbol{G}^T\boldsymbol{K}^{-T}\boldsymbol{R}^T \in R^{n_V \times m}$$

$$\boldsymbol{C} = \boldsymbol{G}^T\boldsymbol{K}^{-T}\boldsymbol{R}^T\boldsymbol{R}\boldsymbol{K}^{-1} \in R^{n_V \times n}, \qquad \boldsymbol{D} = \boldsymbol{K}^{-T}\boldsymbol{R}^T\boldsymbol{R}\boldsymbol{K}^{-1} \in R^{n \times n}$$

$$\boldsymbol{P} = \boldsymbol{R}\boldsymbol{K}^{-1} \in R^{m \times n} \tag{12}$$

Equation (11) gives the square error between the actual and desired shapes, which will be used as an objective or constraint function in the optimization of control voltage distribution in the following sections.

III. Shape Control Subject to Control Energy Constraint

In engineering practice, the energy used in shape control of structures is not unlimited. Therefore, how to perform shape control of a smart structure subject to an energy constraint is of great significance in practice.

For a given control energy E_M and a desire shape $\boldsymbol{y}_d$, the shape control is to find the optimal control voltage distribution whose control energy is not larger than E_M to minimize the square error between the actuated and desired shapes. When Eqs. (9) and (11) are noted, the shape control problem subject to energy constraint can be stated as follows:

$$\text{minimize } e = \boldsymbol{v}^T\boldsymbol{A}\boldsymbol{v} + 2\boldsymbol{v}^T\boldsymbol{B}\boldsymbol{y}_d - 2\boldsymbol{v}^T\boldsymbol{C}\boldsymbol{f} + \boldsymbol{f}^T\boldsymbol{D}\boldsymbol{f} - 2\boldsymbol{y}_d^T\boldsymbol{P}\boldsymbol{f} + \boldsymbol{y}_d^T\boldsymbol{y}_d$$

$$\text{subject to: } z_0\boldsymbol{v}^T\boldsymbol{v} \le E_M \tag{13a}$$

To find the optimal voltage in Eq. (13a) in which an inequality constraint is imposed, we start with investigating the problem with an equality constraint given by

$$\text{minimize } e = \boldsymbol{v}^T\boldsymbol{A}\boldsymbol{v} + 2\boldsymbol{v}^T\boldsymbol{B}\boldsymbol{y}_d - 2\boldsymbol{v}^T\boldsymbol{C}\boldsymbol{f} + \boldsymbol{f}^T\boldsymbol{D}\boldsymbol{f} - 2\boldsymbol{y}_d^T\boldsymbol{P}\boldsymbol{f} + \boldsymbol{y}_d^T\boldsymbol{y}_d$$

$$\text{subject to: } z_0\boldsymbol{v}^T\boldsymbol{v} = E_0 \le E_M \tag{13b}$$

where E_0 is an arbitrary energy.

To find the optimal control voltage $\boldsymbol{v}$ in Eq. (13b), we construct a function using the Lagrangian multiplier λ as

$$g(\boldsymbol{v}, \lambda) = \boldsymbol{v}^T\boldsymbol{A}\boldsymbol{v} + 2\boldsymbol{v}^T\boldsymbol{B}\boldsymbol{y}_d - 2\boldsymbol{v}^T\boldsymbol{C}\boldsymbol{f} + \boldsymbol{f}^T\boldsymbol{D}\boldsymbol{f} - 2\boldsymbol{y}_d^T\boldsymbol{P}\boldsymbol{f} + \boldsymbol{y}_d^T\boldsymbol{y}_d + \lambda\left(z_0\boldsymbol{v}^T\boldsymbol{v} - E_0\right) \tag{14}$$

The optimal voltage distribution can be solved from

$$\frac{\partial g}{\partial \boldsymbol{v}} = 0, \qquad \frac{\partial g}{\partial \lambda} = 0 \tag{15}$$

that is,

$$\boldsymbol{A}\boldsymbol{v} + \boldsymbol{B}\boldsymbol{y}_d - \boldsymbol{C}\boldsymbol{f} + \lambda z_0\boldsymbol{v} = 0 \tag{16a}$$

$$z_0\boldsymbol{v}^T\boldsymbol{v} = E_0 \tag{16b}$$

When

$$\boldsymbol{b} = \boldsymbol{C}\boldsymbol{f} - \boldsymbol{B}\boldsymbol{y}_d \tag{17}$$

is denoted in Eq. (16a), the control voltage $\boldsymbol{v}$ can be expressed as

$$\boldsymbol{v} = (\boldsymbol{A} + \lambda z_0\boldsymbol{I})^{-1}\boldsymbol{b} \tag{18}$$

When Eq. (18) is substituted into Eq. (16b), the following equation of λ can be obtained:

$$z_0\boldsymbol{b}^T(\boldsymbol{A} + \lambda z_0\boldsymbol{I})^{-T}(\boldsymbol{A} + \lambda z_0\boldsymbol{I})^{-1}\boldsymbol{b} - E_0 = 0 \tag{19}$$

Equation (19) is an algebraic equation from which $2n_V$ roots can be solved using root finding algorithms. After finding the roots of Eq. (19), the control voltage can be obtained from Eq. (18) for each λ.

It is evident that solving the Lagrangian multiplier λ is a key step for obtaining the optimal voltage. However, direct search of the roots of Eq. (19) is generally inefficient because of the extensive calculation of an inverse matrix (or solution of a set of simultaneous equations instead) in every iteration step of searching the roots. Therefore, we will derive another equation of λ that is easier to be solved. To this end, express $\boldsymbol{v}$ and $\boldsymbol{b}$ as

$$\boldsymbol{v} = \sum_{i=1}^{n_V}\beta_i\boldsymbol{\varphi}_i, \qquad \boldsymbol{b} = \sum_{i=1}^{n_V}\eta_i\boldsymbol{\varphi}_i \tag{20}$$

where $\boldsymbol{\varphi}_i$, $i = 1, 2, \ldots, n_V$, is the ith eigenvector of the matrix $\boldsymbol{A}$ associated with the ith eigenvalue α_i. Note that $\boldsymbol{\varphi}_i$ and α_i of matrix $\boldsymbol{A}$ are real because it is a positive definite symmetric matrix. In Eq. (20), β_i and η_i are the projections of the vectors $\boldsymbol{v}$ and $\boldsymbol{b}$ on the ith eigenvector, respectively, which are given by

$$\beta_i = \langle \boldsymbol{v}, \boldsymbol{\varphi}_i \rangle = \boldsymbol{v} \cdot \boldsymbol{\varphi}_i, \qquad \eta_i = \langle \boldsymbol{b}, \boldsymbol{\varphi}_i \rangle = \boldsymbol{b} \cdot \boldsymbol{\varphi}_i$$

Substituting Eq. (20) into Eq. (16a), and noting $\boldsymbol{A}\boldsymbol{\varphi}_i = \lambda_i\boldsymbol{\varphi}_i$, we have

$$\sum_{i=1}^{n_V}(\alpha_i\beta_i + \lambda z_0\beta_i - \eta_i)\boldsymbol{\varphi}_i = 0 \tag{21}$$

Because the eigenvectors $\boldsymbol{\varphi}_i$, $i = 1, 2, \ldots, n_V$ are linearly independent, Eq. (21) gives

$$\beta_i = \eta_i/(\lambda z_0 + \alpha_i), \qquad i = 1, 2, \ldots, n_V \tag{22}$$

Substituting Eq. (20) into Eq. (16b) yields

$$\sum_{i=1}^{n_V} z_0\beta_i^2 = E_0 \tag{23}$$

Substituting Eq. (22) into Eq. (23), we have

$$\sum_{i=1}^{n_V}\frac{z_0\eta_i^2}{(\lambda z_0 + \alpha_i)^2} - E_0 = 0 \tag{24}$$

Equation (24) has an explicit form for the unknown λ, which can be used to replace Eq. (19). The roots of Eq. (24) appear either as real ones or as conjugate pairs. The main advantage of using Eq. (24) instead of Eq. (19) is that it does not need to calculate an inverse of a matrix (or solve a simultaneous equations) in every step in the root searching process. The eigenvalues and eigenvectors of the real positive-definite matrix $\boldsymbol{A}$ are needed to be solved once before solving Eq. (24), and therefore, the computing load for finding Lagrangian multiplier λ from Eq. (24) is dramatically reduced than that from Eq. (19). After finding all λ from Eq. (24), $2n_V$ voltage vectors for each λ can be obtained from Eqs. (20) and (22), that is,

$$\boldsymbol{v}_j = \sum_{i=1}^{n_V}\frac{\eta_i}{\lambda_j z_0 + \alpha_i}\boldsymbol{\varphi}_i, \qquad j = 1, 2, \ldots, 2n_V \tag{25}$$

Among the $2n_V$ voltage vectors, there is one voltage distribution that makes the square error e minimum. It can be seen from Eq. (16a) that only the real ones from the $2n_V$ roots of Eq. (19) or Eq. (24) can result in reasonable control voltage distributions. In addition, when $\lambda = 0$, Eq. (16a) will give an optimal voltage distribution without energy constraint. Therefore, we can conclude that the real Lagrangian multiplier λ with smallest absolute value will gives the optimal control voltage distribution. The global optimal energy (without any energy constraint) can be solved directly from Eq. (24). Substituting $\lambda = 0$ into Eq. (24), one can obtain the global optimal energy as

$$E_g = \sum_{i=1}^{n_V}\frac{z_0\eta_i^2}{\alpha_i^2} \tag{26}$$

which means that there does exist control energy E_g, which makes one of the Lagrangian multipliers zero. When $\lambda = 0$ is substitued into Eq. (25), the global optimal (minimum) square error is obtained as

$$\boldsymbol{v}_g = \sum_{i=1}^{nV} \frac{\eta_i}{\alpha_i} \varphi_i \tag{27}$$

Based on monotone analysis of the relationship between the optimal square error and the control energy E_0 from Eq. (13b), the optimal square error constrained by an inequality condition in Eq. (13a) can also be determined.

IV. Shape Control as Least Control Energy Subject to Square Error Tolerance Constraint

In shape control of structures, it is important to find a possible cost-effective way to achieve the desired shape within a given tolerable error e_M. Such a problem can be described as

$$\text{minimize } z_0 \boldsymbol{v}^T \boldsymbol{v}$$

$$\text{subject to: } \boldsymbol{v}^T \boldsymbol{A} \boldsymbol{v} - 2\boldsymbol{v}^T \boldsymbol{b} + \boldsymbol{f}^T \boldsymbol{D} \boldsymbol{f} - 2\boldsymbol{y}_d^T \boldsymbol{P} \boldsymbol{f} + \boldsymbol{y}_d^T \boldsymbol{y}_d \leq e_M \tag{28a}$$

Similarly, before finding the optimal voltages from Eq. (28a), we consider

$$\text{minimize } z_0 \boldsymbol{v}^T \boldsymbol{v}$$

$$\text{subject to: } \boldsymbol{v}^T \boldsymbol{A} \boldsymbol{v} - 2\boldsymbol{v}^T \boldsymbol{b} + \boldsymbol{f}^T \boldsymbol{D} \boldsymbol{f} - 2\boldsymbol{y}_d^T \boldsymbol{P} \boldsymbol{f} + \boldsymbol{y}_d^T \boldsymbol{y}_d = e_0 \leq e_M \tag{28b}$$

where e_0 is an arbitrarily designated square error.

When the same procedure in Sec. III is followed, the optimal voltage distribution can be found from

$$(z_0 \boldsymbol{I} + \lambda \boldsymbol{A}) \boldsymbol{v} - \lambda \boldsymbol{b} = 0$$

$$\boldsymbol{v}^T \boldsymbol{A} \boldsymbol{v} - 2\boldsymbol{v}^T \boldsymbol{b} + \boldsymbol{f}^T \boldsymbol{D} \boldsymbol{f} - 2\boldsymbol{y}_d^T \boldsymbol{P} \boldsymbol{f} + \boldsymbol{y}_d^T \boldsymbol{y}_d = e_0 \tag{29}$$

Substituting Eq. (20) into the first equation in Eq. (29), we have

$$\sum_{i=1}^{nV} (\lambda \alpha_i \beta_i + z_0 \beta_i - \lambda \eta_i) \varphi_i = 0 \tag{30}$$

and, hence, β_i can be expressed as

$$\beta_i = \lambda \eta_i / (z_0 + \lambda \alpha_i), \qquad i = 1, 2, \ldots, n_V \tag{31}$$

Substituting Eq. (20) into the second equation in Eq. (29) gives

$$\sum_{i=1}^{nV} \alpha_i \beta_i^2 - 2 \sum_{i=1}^{nV} \beta_i \eta_i - e_r = 0 \tag{32}$$

where

$$e_r = e_0 - \boldsymbol{f}^T \boldsymbol{D} \boldsymbol{f} + 2\boldsymbol{y}_d^T \boldsymbol{P} \boldsymbol{f} - \boldsymbol{y}_d^T \boldsymbol{y}_d \tag{33}$$

Substituting Eq. (31) into Eq. (32) yields

$$\sum_{i=1}^{nV} \left[\frac{\lambda^2 \alpha_i \eta_i^2}{(z_0 + \lambda \alpha_i)^2} - \frac{2\lambda \eta_i^2}{z_i + \lambda \alpha_i} \right] - e_r = 0 \tag{34}$$

Equation (34) is an equation of the unknown λ, from which we can obtain $2n_V$ real and complex roots. Only the real roots of Eq. (34) can give real voltages, as indicated in Eqs. (20) and (31). After finding the Lagrangian multipliers λ by solving Eq. (34), we can obtain the voltage vector using Eqs. (31) and (20) for each λ, and then the optimal voltage distribution $\boldsymbol{v}_{\text{opt}}$ can be found among all of the voltage vectors.

Note that Eq. (34) will not have any real roots if the given error e_0 is very small. This means that the given small error cannot be implemented. If an achievable error e_0 is given, Eq. (34) will have one or more real roots, which will give one or more voltage distributions to achieve the given error and one with least energy among them. This indicates that the control voltage distribution for shape control is not unique if the square error defined in Eq. (8) is used to measure the closeness of the actuated and desired shapes.

For a number of prescribed square errors e_0, the related optimal control energy E_{opt} can be obtained from Eq. (28b). By the examination of the monotone of the relationship between the square error and its corresponding optimal energy, the optimal energy can be obtained for Eq. (28a).

V. Examples

As an example, consider a cantilever rectangular plate in a horizontal plane bonded with 20 rectangular piezoelectric actuator patches on its upper surface, as shown in Fig. 1. The geometrical dimensions of the host plate are $0.15 \times 0.12 \times 0.001$ m^3 and those of each piezoelectric actuator are $0.02 \times 0.02 \times 0.0005$ m^3. The gap between two actuator patches is 0.01 m, and the gap between the actuator patches to the edge is 0.005 m. The physical properties of the aluminum host plate are $E_1 = E_2 = 68.9$ GPa, $\mu_{12} = \mu_{23} = 0.25$, and $\rho = 2700$ kg/m^3. The piezoelectric material has the following properties: $E_1 = E_2 = 81.3$ GPa, $\mu_{12} = \mu_{23} = 0.43$, $\rho = 7600$ kg/m^3, $e_{31} = e_{32} = -9.52$ N/Vm, $e_{15} = e_{24} = 0$, and other entries in the piezoelectric stress matrix are zero. The control voltage is uniformly distributed in each piezoelectric actuator, and the electric conductance for the actuators is assumed to be $z_0 = 1.0$.

In this example, an adhesive element is employed to form the basic equations of the composite plate, which includes both peel and shear effects in the adhesive layer based on the first-order shear deformation plate theory.[20] In the FEA, the thin adhesive layer between the piezoelectric layer and the host plate is modeled by assuming that it carries constant shear and peel strains throughout its thickness. Four-node isoparametric elements with five DOF at each node are used. The adhesive layer between each actuator patch and the host plate is taken as 0.15 mm, and its physical properties are $E_1 = E_2 = 2.4$ GPa, $\mu_{12} = \mu_{23} = 0.34$, $\rho = 1600$ kg/m^3, and $g = 9.80$ m/s^2. The composite plate is divided into 99 elements and each actuator patch is modeled by one element.

In this example, the desired shape is chosen as

$$w(x, y) = (\cosh x - 1) \sin y/2$$

$$0 \leq x \leq 0.15, \qquad -0.06 \leq y \leq 0.06$$

which resembles a twisted wing structure. We choose the transverse displacements at all nodes in the host plate as the objective index, that is, the subweighting matrices corresponding to the nodes of the piezoelectric actuators are set to be zero. In the subweighting matrices for the nodes of the host plate, only the weighting coefficient

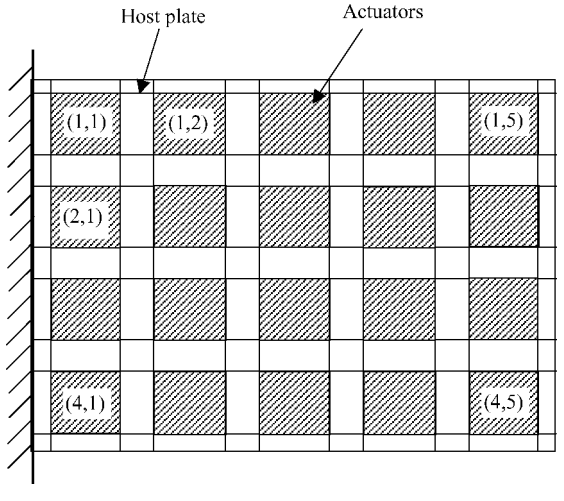

Fig. 1 Cantilever plate with 20 piezoelectric actuator patches (99 elements).

R_{wi} is selected to be 1.0, whereas the other four coefficients are zeros.

Case 1: Static Shape Control with Given Control Energy

First, we examine the relationship between the given control energy and the related optimal square error. The global optimal control energy obtained from Eq. (26) is $E_g = 5.624 \times 10^8$, and the global optimal square error is $e_g = 3.205 \times 10^{-8}$, which are actually the same with those obtained without energy constraint. When the control energy E_0 is assigned with different values, the constrained optimal square errors obtained from Eq. (13b) are shown in Fig. 2, in which the optimal square error is normalized by the $e_g(e_{\text{opt}}/e_g \times 100)$ and the control energy is also normalized by $E_g(E_0/E_{\text{opt}} \times 100)$. It is clearly shown that the optimal square error-energy curve decreases monotonically at the interval $[0, E_g]$ and it increases monotonically with the control energy when $E_0 > E_g$. With the optimal square error-energy curve, the optimal square error for limiting the control energy within a given range, as described in Eq. (13a), can also be determined. In one case where the control energy is limited within a value $E_M < E_g$, the optimal square error will be achieved at the energy boundary, that is, at $E = E_M$, as shown in Fig. 2. In the second case, if the energy limitation E_M assigned is higher than E_g, that is, $E_M \geq E_g$, the optimal square error will be achieved at $E = E_g$. The first case is more interesting in engineering practice.

Next, we investigate the voltage distribution among the 20 actuator patches constrained by a given control energy. When the control energy is taken as $E_0 = 3.2 \times 10^8$, the optimal control voltage obtained from Eqs. (22) and (25) is listed in Table 1. In this case, the square error between the actual and desired shape is $e = 3.870 \times 10^{-8}$, and the actuated shape of the plate by the obtained control voltage is shown in Fig. 3. The global optimal voltage obtained from Eq. (27) is also presented in Table 1. In this case, the required control energy $E_g = 5.624 \times 10^8$, and the minimum square error obtained from Eq. (30) is $e_g = 3.205 \times 10^{-8}$. To show

Table 1 Values of applied voltages for the case with and without energy constraint

Row	Column 1	Column 2	Column 3	Column 4	Column 5
1	−5341.7	−8100.7	−5982.1	−5426.6	901.8
	(−5094.5)[a]	(−5924.5)	(−4877.9)	(−3950.2)	(1555.6)
2	−2749.9	5973.4	4282.7	2681.5	657.9
	(−645.7)	(2639.3)	(2430.9)	(1048.7)	(585.1)
3	8836.3	−5335.2	−3817.7	−2689.7	−1184.5
	(4766.5)	(−2153.9)	(−2419.7)	(−1061.4)	(−1317.5)
4	3665.5	9916.7	7047.2	6379.8	−1037.8
	(5476.1)	(8208.6)	(6427.9)	(4987.2)	(−1660.9)

[a]Numbers in parentheses are results for the case with constraint.

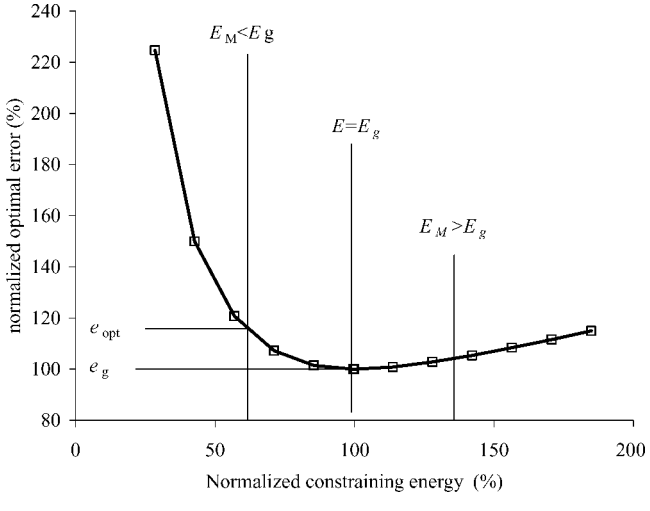

Fig. 2 Optimal square error vs constraining energy.

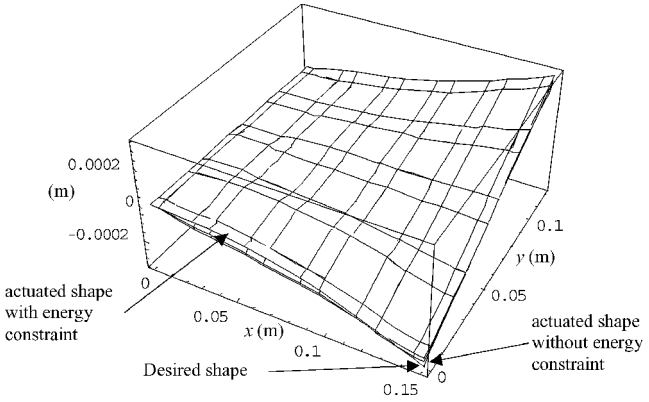

Fig. 3 Transverse displacements of plate.

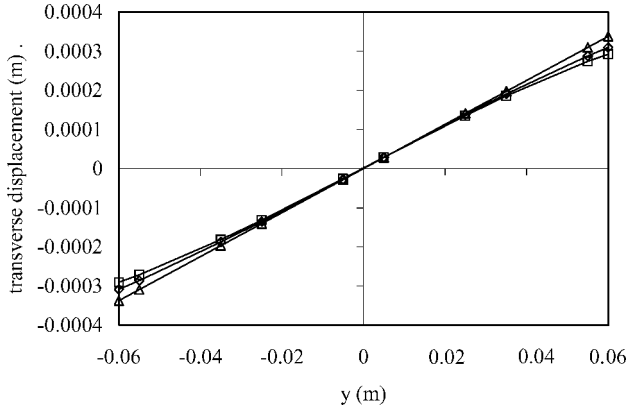

Fig. 4 Transverse displacements at edge $x = 0.15$ m: □, energy constrained; ◇, no energy constraint; and △, desired.

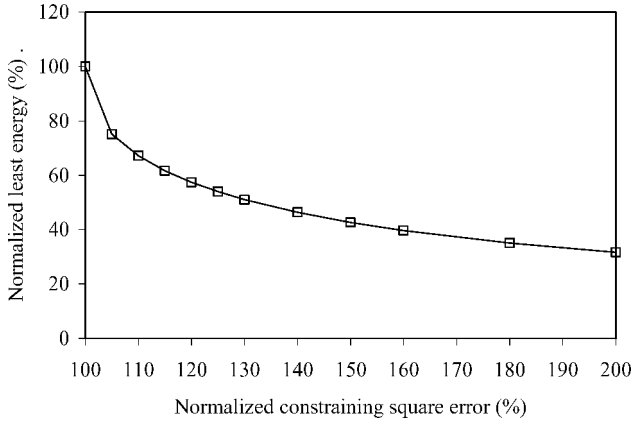

Fig. 5 Least energy vs constraining square error.

the error between the shape with and without energy constraint, the transverse displacements at the edge $x = 0.15$ m are given in Fig. 4. As shown in Figs. 2 and 3, with energy constraint, the square error between the actual and desired shapes is larger than that without energy constraint.

Case 2: Static Shape Control with Least Control Energy

First, we examine the relationship between the given square error and the related least control energy. For any given error e_0 in Eq. (28b), a least control energy can be found from Eqs. (20), (29), and (32), and a least control energy-constraining curve is given in Fig. 5. In Fig. 5, the error and control energy are also normalized using the minimum error e_g and the global optimal control energy E_g respectively. The least control energy-constraining curve is decreasing monotonous. When the square error is constrained by an inequality equation $e \leq e_M$, as given in Eq. (28a), the least control

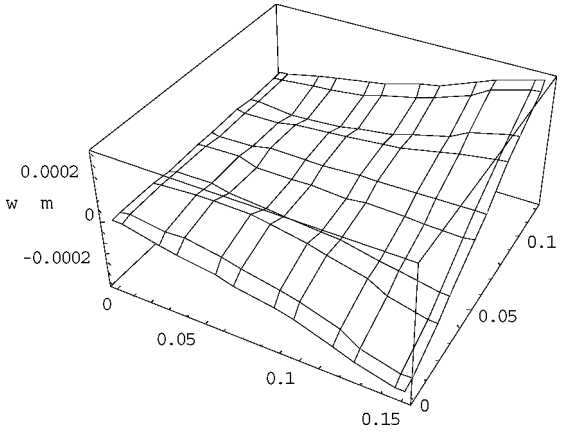

a) E = 75.17% E_g

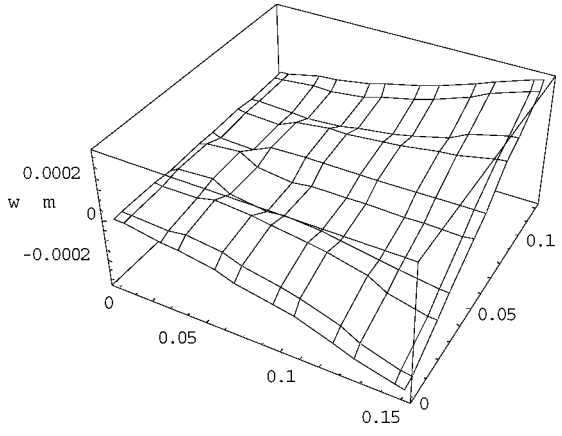

b) E = 140.2% E_g

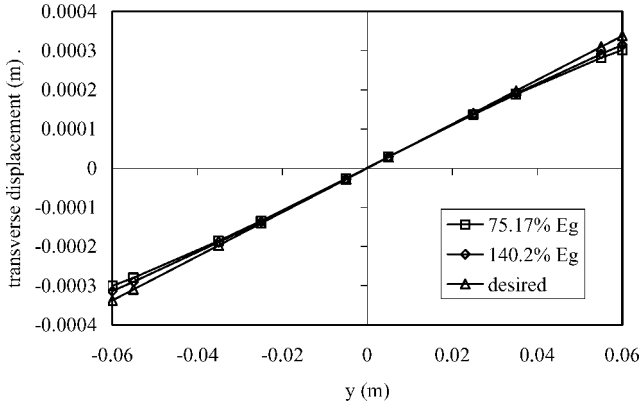

c) Deflection at the free end of the plate, y = 0.15 m

Fig. 6 Shapes with the same square error but actuated by different voltage distributions.

energy will be always achieved at $e = e_m$. In other words, the least energy is the one used to achieve the shape with maximum permissible error.

In addition, as shown in Fig. 5, as the error decreases, the least control energy needed to achieve the desired error increases nonlinearly. When the given error is close to the minimum square error, to decrease the error further will need much more control energy than that when the given error is far from the minimum error. For example, if the error increases 10% at 150% of the minimum error, the requested least control energy will decrease 7%. However, if the error decreases by the same percent from 100% of the minimum error, the least control energy will significantly decreases 32.8%.

Finally, we check the voltage distribution to achieve the shape with a designated square error. For a given square error $e_0 = 105\% e_g = 3.365 \times 10^{-8}$, Eq. (34) has two real roots, and hence,

Table 2 Two possible voltage distributions for $e_0 = 105\%, e_g = 3.365 \times 10^{-8}$

Row	Column 1	Column 2	Column 3	Column 4	Column 5
1	−5372.3[a]	−6996.7	−5475.02	−4742.5	1270.1
	(−4222.8)	(−8880.3)	(−6176.5)	(−5839.0)	(624.9)
2	−1075.5	4192.9	3565.0	1812.9	611.3
	(−7207.6)	(7588.8)	(4120.3)	(3407.0)	(674.5)
3	5964.1	−3686.8	−3403.8	−1807.9	−1273.0
	(14378.4)	(−6796.6)	(−3359.7)	(−3443.2)	(−1070.7)
4	4951.0	9147.1	6839.1	5763.3	−1397.4
	(1410.9)	(10345.4)	(6978.6)	(6712.1)	(−753.1)

[a]Numbers without parentheses are results with least control energy.

two voltage distributions can be obtained and listed in Table 2. The control energy for these two distributions is 75.17% and 140.20% of the optimal one, respectively, which can also be found in Fig. 2. In this case, the least control energy is 75.17% of the optimal one and the 20 voltages are −5372.3, −1075.51, 5964.17, 4951, −6996.73, 4192.99, −3686.88, 9147.09, −5475.03, 3565.03, −3403.82, 6839.07, −4742.57, 1812.9, −1807.92, 5763.28, 1270.15, 611.332, −1272.95 and −1397.37 V, respectively, whereas the control voltage distribution with 140.20% of the optimal energy is −4222.82, −7207.47, 14,378.2, 1410.96, −8880.25, 7588.72, −6796.58, 10,345.4, −6176.46, 4120.28, −3359.71, 6978.66, −5839.01, 3406.94, −3443.21, 6712.04, 624.944, 674.502, −1070.74 and −753.096 V, respectively. The shapes actuated by these two voltage distributions are presented in Fig. 6. It can be seen from Fig. 6 that these two shapes are different although they have the same square error.

VI. Conclusions

Static shape control of structures subject to two different constraints is investigated. An efficient scheme is presented for finding the energy-constrained optimal voltage distribution for piezoelectric actuator patches. The voltage distribution with optimal energy to achieve the desired shape at a designated error tolerance is also obtained. The simulation examples show that the energy constraint can significantly affect the shape control effect. If the control energy is limited in a proper range around an optimal value, good control results can be achieved, whereas the control energy far from the optimal one leads to a big error between the actuated the desired shape, especially for lower control energy. It is also observed that much more control energy is needed to achieve a desired shape at a very small error tolerance than that at a slightly larger one.

In engineering practice, in addition to the control energy constraint, the control voltage on each actuator should be limited in a proper range because very high voltage will lead to depolarization of the actuator. Thus, combining energy-constrained shape control and voltage constraints will give more practical control voltage distribution in static shape control of flexible structures.

Acknowledgment

The authors are grateful to the support of the Australian Research Council via Discovery-Projects Grant (Grant DP0210716).

References

[1]Haftka, R. T., and Adelman, H. M., "An Analytical Investigation of Shape Control of Large Space Structures by Applied Temperatures," *AIAA Journal*, Vol. 23, No. 3, 1985, pp. 450–457.

[2]Paradies, R., Hertwig, M., and Elspass, W. J., "Shape Control of an Adaptive Mirror at Different Angles of Inclination," *Journal of Intelligent Material Systems and Structures*, Vol. 7, No. 2, 1996, pp. 203–210.

[3]Balas, M. J., "Optimal Quasi-Static Shape Control for Large Aerospace Antennae," *Journal of Optimization Theory and Applications*, Vol. 46, No. 2, 1985, pp. 153–170.

[4]Austin, F., Rossi, M. J., Vannostrand, W., Knowles, G., and Jameson, A., "Static Shape Control for Adaptive Wings," *AIAA Journal*, Vol. 32, No. 9, 1994, pp. 1895–1901.

[5]Agrawal, S. K., Tong, D. Q., and Nagaraja, K., "Modeling and Shape Control of Piezoelectric Actuator Embedded Elastic Plates," *Journal of Intelligent Material Systems and Structures*, Vol. 5, No. 4, 1994, pp. 514–521.

[6]Ghosh, K. G., and Batra, R. C., "Shape Control of Plates Using Piezoceramic Elements," *AIAA Journal*, Vol. 33, No. 7, 1995, pp. 1354–1357.

[7]Batra, R. C., Liang, X. Q., and Yang, J. S., "Shape Control of Vibrating Simply Supported Rectangular Plates," *AIAA Journal*, Vol. 34, No. 1, 1996, pp. 116–122.

[8]Bruch, J. C., Sloss, J. M., Adali, S., and Sadek, I. S., "Optimal Piezoactuator Locations/Lengths and Applied Voltage for Shape Control of Beams," *Smart Materials and Structures*, Vol. 9, No. 2, 2000, pp. 205–211.

[9]Lawson, C., and Hanson, R., *Solving Least Squares Problems*, Prentice–Hall, Upper Saddle River, NJ, 1974, pp. 107–158.

[10]Watson, L. T., Haralick, R. M., and Zuniga, O. A., "Constrained Transform Coding and Surface Fitting," *IEEE Transaction on Communications*, Vol. 31, No. 5, 1983, pp. 717–726.

[11]Kapuria, S., Sengupta, S., and Dumir, P. C., "Three-Dimensional Piezothermoelastic Solution for Shape Control of Cylindrical Panel," *Journal of Thermal Stresses*, Vol. 20, No. 1, 1997, pp. 67–85.

[12]Yang, S. Y., and Ngoi, B., "Shape Control of Beams by Piezoelectric Actuators," *AIAA Journal*, Vol. 38, No. 12, 2000, pp. 2292–2298.

[13]Koconis, D. B., Kollar, L. P., and Springer, G. S., "Shape Control of Composite Plates and Shells with Embedded Actuators. 2. Desired Shape Specified," *Journal of Composite Materials*, Vol. 28, No. 5, 1994, pp. 459–482.

[14]Hsu, C. Y., Lin, C. C., and Gaul, L., "Shape Control of Composite Plates by Bonded Actuators with High Performance Configuration," *Journal of Reinforced Plastics and Composites*, Vol. 16, No. 18, 1997, pp. 1692–1710.

[15]Onoda, J., and Hanawa, Y., "Actuator Placement Optimization by Genetic and Improved Simulated Annealing Algorithms," *AIAA Journal*, Vol. 31, No. 6, 1993, pp. 1167–1169.

[16]Agrawal, B. N., and Treanor, K. E., "Shape Control of a Beam Using Piezoelectric Actuators," *Smart Materials and Structures*, Vol. 8, No. 6, 1999, pp. 729–739.

[17]Chee, C. Y. K., Tong, L. Y., and Steven, G. P., "Static Shape Control of Composite Plates Using a Slope-Displacement-Based Algorithm," *AIAA Journal*, Vol. 40, No. 8, 2002, pp. 1611–1618.

[18]Irschik, H., "A Review on Static and Dynamic Shape Control of Structures by Piezoelectric Actuation," *Engineering Structures*, Vol. 24, No. 1, 2002, pp. 5–11.

[19]Chee, C. Y. K., Tong, L. Y., and Steven, G. P., "Static Shape Control of Composite Plates Using a Curvature-Displacement Based Algorithm," *International Journal of Solids and Structures*, Vol. 38, No. 36–37, 2001, pp. 6381–6403.

[20]Sun, D. C., and Tong, L. Y., "Adhesive Element Modeling and Weighted Static Shape Control of Composite Plates with Piezoelectric Actuator Patches," *International Journal for Numerical Methods in Engineering* (to be published).

A. Berman
Associate Editor